

Detecting habitat preferences and monitoring population dynamics of sea cucumbers in coastal ecosystems through underwater photogrammetry

*Original*

Detecting habitat preferences and monitoring population dynamics of sea cucumbers in coastal ecosystems through underwater photogrammetry / Ventura, Daniele; Rakaj, Arnold; Lasinio, Giovanna Jona; Sangiovanni, Gian Mario; Poggio, Daniele; Mastrantonio, Gianluca; Pollice, Alessio; Grasso, Gaia; Casoli, Edoardo; Mancini, Gianluca; Pace, Daniela Silvia; Mohan, Midhun; Valente, Tommaso; Belluscio, Andrea; Ardizzone, Giandomenico; Moro, Stefano. - In: JOURNAL OF ENVIRONMENTAL MANAGEMENT. - ISSN 1095-8630. - ELETTRONICO. - 377:(2025), pp. 1-13.

[10.1016/j.jenvman.2025.124589]

*Availability:*

This version is available at: 11583/2998047 since: 2025-03-04T14:10:16Z

*Publisher:*

Elsevier

*Published*

DOI:10.1016/j.jenvman.2025.124589

*Terms of use:*

This article is made available under terms and conditions as specified in the corresponding bibliographic description in the repository

*Publisher copyright*

(Article begins on next page)



## Research article

# Detecting habitat preferences and monitoring population dynamics of sea cucumbers in coastal ecosystems through underwater photogrammetry

Daniele Ventura<sup>a,\*</sup>, Arnold Rakaj<sup>b,c</sup>, Giovanna Jona Lasinio<sup>d</sup>, Gian Mario Sangiovanni<sup>d</sup>, Daniele Poggio<sup>e</sup>, Gianluca Mastrantonio<sup>e</sup>, Alessio Pollice<sup>f</sup>, Gaia Grasso<sup>g</sup>, Edoardo Casoli<sup>a</sup>, Gianluca Mancini<sup>a</sup>, Daniela Silvia Pace<sup>a</sup>, Midhun Mohan<sup>h</sup>, Tommaso Valente<sup>a,i</sup>, Andrea Belluscio<sup>a</sup>, Giandomenico Ardizzone<sup>a</sup>, Stefano Moro<sup>j</sup>

<sup>a</sup> Department of Environmental Biology, University of Rome 'La Sapienza', V. le dell'Università 32, 00185, Rome, Italy

<sup>b</sup> Experimental Ecology and Aquaculture Laboratory, Department of Biology, University of Rome Tor Vergata, Via della Ricerca Scientifica, 00133, Rome, Italy

<sup>c</sup> National Inter-University Consortium for Marine Sciences-CoNISMa, Rome, Italy, Rome, Italy

<sup>d</sup> Department of Statistical Sciences, University of Rome 'La Sapienza', P.le Aldo Moro 5, 00185, Rome, Italy

<sup>e</sup> Department of Mathematical Sciences 'G. L. Lagrange', Politecnico di Torino, Corso Duca degli Abruzzi, 24, 10129, Torino, Italy

<sup>f</sup> Department of Economics and Finance, Università degli Studi di Bari Aldo Moro, Largo Abbazia Santa Scolastica, 70124, Bari, Italy

<sup>g</sup> Department of Integrative Marine Ecology (EMI), Stazione Zoologica Anton Dohrn, Via Francesco Buonocore 42, 80077, Ischia, Italy

<sup>h</sup> Ecoresolve, San Francisco, CA, United States

<sup>i</sup> Italian National Institute for Environmental Protection and Research (ISPRA), Via del Fosso di Fiorano 64, Roma, RM, 00143, Italy

<sup>j</sup> Department of Integrative Marine Ecology (EMI), Stazione Zoologica Anton Dohrn, Via Gregorio Allegri 1, 00198, Rome, Italy

## ARTICLE INFO

## Keywords:

SfM

VRM

Benthic habitats

Seagrass meadows

*Holothuria tubulosa*

Mediterranean Sea

LGCP

## ABSTRACT

Sea cucumbers constitute common benthic organisms in the subtidal zones capable of providing key ecosystem services. Due to the recent harvesting and increased commercial interest in Mediterranean species, fundamental ecological knowledge is required to promote adequate management measures. In this regard, a remotely sensed mapping method is proposed for deriving length-frequency distribution and defining habitat preferences of a common sea cucumber species. Image analyses and classification carried out on high spatial resolution cartographic products, including orthophoto mosaics and digital surface models derived by 'Structure-from-Motion' photogrammetric processing, allowed accurate estimation of sea cucumber densities over an area of 5500 m<sup>2</sup>. The mean length of mapped specimens ranged from 8 to 50 cm, with a peak in abundance recorded in April. A distinct preference for sandy substrates was observed, characterized by low vector ruggedness measure values ranging from 0 to 0.15. A negative correlation was also identified in areas with slopes exceeding 15°, especially among larger size classes. Spatial patterns investigated with a Log-Gaussian Cox Process showed significant temporal trends with well-defined aggregation patterns during the summer months in specific areas covered by transplanted *P. oceanica* fragments with higher (up to 0.25) vector ruggedness measure values. This finding confirmed the essential role of this restored habitat in retaining fine organic particle used as a source of food for deposit-feeding holothurians. This approach is expected to enhance the creation of tailored management plans for sea cucumber populations in coastal regions, facilitating accurate assessments of the impacts of fishing activities on these species.

## 1. Introduction

Deposit-feeding holothurians (Echinodermata, Holothuroidea), commonly known as sea cucumbers, are a large group of marine benthic invertebrates distributed worldwide. They occupy various niches in almost every benthic zone of the marine environment, ranging from the

intertidal to the abyssal regions (Mercier et al., 2024). On a global scale, sea cucumbers constitute some of the most common benthic organisms in the intertidal and subtidal zones, representing most of the total biomass in slope and abyssal benthic ecosystems (Purcell et al., 2023). Although most sea cucumbers are either stationary or move at a slow pace (Uthicke and Benzie, 2001), the presence of these organisms plays a

\* Corresponding author.

E-mail address: [daniele.ventura@uniroma.it](mailto:daniele.ventura@uniroma.it) (D. Ventura).

<https://doi.org/10.1016/j.jenvman.2025.124589>

Received 26 January 2025; Received in revised form 14 February 2025; Accepted 14 February 2025

Available online 20 February 2025

0301-4797/© 2025 The Authors. Published by Elsevier Ltd. This is an open access article under the CC BY license (<http://creativecommons.org/licenses/by/4.0/>).

crucial role in influencing the physicochemical dynamics of soft bottom, reef ecosystems, and seagrass meadows, being directly involved in sediment bioturbation and nutrient recycling during their feeding activities (Lopez and Levinton, 1987). Bioturbation performed by holothurians provides essential ecosystem services that enhance local productivity, diminish organic load, mitigate stratification and sediment nitrification, redistribute surface sediments, and liberate nutrients sequestered in the upper sediment layer (Purcell et al., 2016a). These processes not only make these nutrients accessible to ecosystems but also promote the productivity of benthic organisms (Williamson et al., 2021). High densities of holothurians determine an overall positive effect on the gross productivity of microalgal communities, which benefit, despite constituting one of the primary food sources of holothuroids, from the nutrient increase caused by bioturbation (Hammond et al., 2020). Several studies indicate that sediment digestion by holothurians may be responsible for up to 50% of the dissolution of  $\text{CaCO}_3$  in reef systems, an essential process as the majority of calcium carbonate on coral reefs is stored in sediment, facilitating the growth of scleractinian corals (Wolfe and Byrne, 2017).

Sea cucumbers are considered an important food source in Asia, where their dried forms are considered a culinary delicacy known as ‘trepang’ or ‘bêche-de-mer’ (Hamel et al., 2024). Furthermore, these organisms also have considerable demand in traditional medicine, cosmetics, and nutraceuticals. Commercially exploited sea cucumbers provide income to millions of coastal fishers worldwide and nutrition to more than 1 billion Asian consumers (Purcell et al., 2025). The high cost of bêche-de-mer, the dried body wall of sea cucumbers (prices depend on the quality of product, size, and species, and can usually oscillate between 50 and 450 US\$  $\text{kg}^{-1}$  but also reached 3000 US\$  $\text{kg}^{-1}$  in some Chinese markets) coupled with the numerous medical applications of sea cucumbers, have led to the overexploitation of most of the Indo-Pacific species (González-Wangüemert et al., 2014; Hamel et al., 2022).

The harvesting of sea cucumbers for commercial purposes has resulted in a decline of this marine resource in the conventional fishing areas near Asia, as well as the emergence of this practice in previously unexplored and remote fishing grounds, including isolated parts of the Pacific, the Galapagos Islands, Chile, and the Russian Federation (Purcell et al., 2012). In tropical and subtropical regions, the long-lasting exploitation of holothurian species inhabiting coral reefs has encouraged global overfishing of many commercial stocks, leading to the development of management strategies relying on fisheries (Ram et al., 2016) and aquaculture (Rakaj et al., 2018, 2021). Due to the increasing market demand, sea cucumber fishery has recently shifted towards emergent target species from the NE Atlantic and the Mediterranean Sea (Dereli and Aydin, 2021; Felix et al., 2024; Sicuro and Levine, 2011). Basic knowledge of the species or population’s biology, ecology, life-history traits, and demographics is needed to promote adequate management measures and effective decisions regarding fishing policies. The vulnerability of these holothurians to overfishing is due not only to overexploitation and weak management but also to severe knowledge gaps on the fundamental ecological traits of these species (Pasquini et al., 2022; Rakaj and Fianchini, 2024).

While several studies (Hammond et al., 2020; Purcell et al., 2016b, 2023; Uthicke, 2001) have investigated the ecological characteristics of holothurians within reef ecosystems, the distribution, abundance, movement patterns, and habitat use of sea cucumbers in the Mediterranean Sea have not been thoroughly investigated.

Monitoring such benthic organisms can be challenging, primarily due to their cryptic behaviour, patchy distribution, and high body flexibility, which can be reshaped according to the habitat characteristics. Therefore, the most widely used non-destructive sampling techniques for studying sea cucumbers’ ecology are based on snorkelling or self-contained underwater breathing apparatus (SCUBA) visual census (Azevedo e Silva et al., 2023; Félix et al., 2024) and mark/recapture techniques (Purcell et al., 2016b; Siegenthaler et al., 2015). In the last

decade, advancements in remote sensing technologies have been integrated into marine research, leading to a notable enhancement in bathymetric data resolution. Among these methods, ‘Structure-from-Motion’ (SfM) photogrammetry represents a powerful tool for accurately mapping the distribution of organisms living in shallow waters (Bayley and Mogg, 2020; Burns et al., 2016; Piazza et al., 2019; Price et al., 2019; Ventura et al., 2023). Recent developments in Uncrewed Aerial Vehicles (UAVs) applications and the implementation of robust Structure-from-Motion algorithms have created new possibilities for conducting observations on a broader scale than traditional underwater direct surveys. These advancements also address various limitations associated with conventional methods, such as elevated costs, inaccuracies, and biases stemming from the observer’s experience (Kilfoil et al., 2020; Li et al., 2021; Williamson et al., 2021).

Despite the initial conservation efforts, there is a growing demand among ecologists, environmental managers, and local stakeholders for precise data on Mediterranean Sea cucumber species. Hence, the main objectives of the present study are: (i) to present a new monitoring technique based on underwater Structure-from-Motion-based imagery which enables fine-scale mapping of benthic habitats and extensive data collection on species distribution; ii) to characterize the habitat requirements for sea cucumbers inhabiting a complex underwater area up to 25 m depth; iii) to present a practical modelling approach for analysing spatial data obtained from abundance estimates of sea cucumbers derived from ortho-rectified photomosaics image analysis.

## 2. Material and methods

### 2.1. Studied species

*Holothuria tubulosa* (Gmelin, 1788), *Holothuria poli* (Delle Chiaje, 1923), and *Holothuria mammata* (Grube, 1840) are common infralittoral sea cucumber species of the Mediterranean Sea, inhabiting soft bottoms with abundant organic matter and *Posidonia oceanica* (Linnaeus) Delile, 1813 meadows. The removal due to overfishing can result in diminished ecosystem functionality, often leading to loss of ecosystem services in the affected areas, potentially creating cascading effects in other coastal environments (Félix et al., 2024). Consequently, in 2018, the Italian Ministry of Agriculture, Food and Forestry issued Ministerial Decree 156/2018, which effectively prohibits sea cucumber fishing along the national coastline (Pasquini et al., 2022). Nevertheless, despite the implemented protective measures, Illegal, Unreported and Unregulated fishing, driven by heightened demand in Asian markets, along with water pollution and habitat degradation, is likely to have a detrimental impact on the natural populations (Vafidis and Antoniadou, 2023). Given that the accurate identification of these species relies on a thorough assessment of their physical attributes, including form, colour, and shape, as well as anatomical features such as the calcareous ring and the presence or absence of Cuvierian tubules, the broad term ‘sea cucumbers’ (*Holothuria* spp.) will be used in this study. This decision was influenced by the limitations imposed by underwater remote sensing imagery, which hindered the identification at the species level. To overcome this limitation and to gather data on species composition, four underwater visual census (UVC) campaigns were carried out during both winter and summer seasons. These campaigns involved three scientific divers who evaluated the relative abundance of the three species throughout the study area, employing two strip transects measuring 100 m  $\times$  3 m.

### 2.2. Study site

Photogrammetric surveys of the seabed were carried out along the northeastern coast of Giglio Island (Central Tyrrhenian Sea, Italy), within the impacted site (south to Punta Gabbianara) by the Costa Concordia shipwrecking (Fig. 1). The area extending for approximately 5000 m<sup>2</sup> from 8 to 27 m of depth, has undergone several disturbance

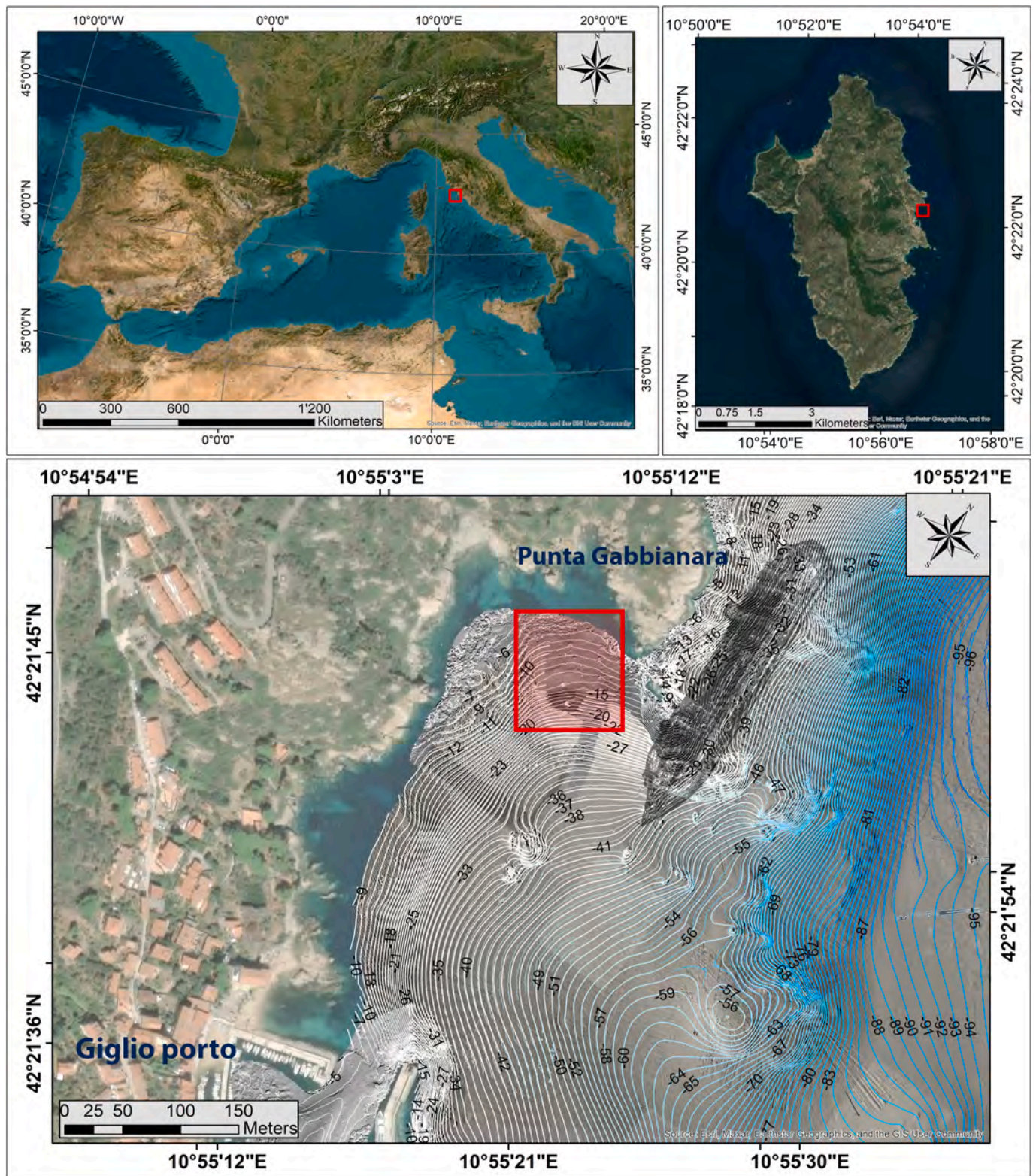


Fig. 1. Geolocalization of the study area (red polygon) along the NE coast of Giglio Island (Tuscany archipelago, Italy). In light grey, the shape of the Costa Concordia shipwreck is reported as a reference. The hillshade relief and contours report the morpho-bathymetrical features of the area.

events, due to the presence of the wreck and the subsequent removal activities (Mancini et al., 2019). In particular, the shadow effect caused by various structures (i.e., wreck and operating vessels) and the sedimentation derived by scraping activity for platform installation severely damaged the natural *Posidonia oceanica* meadow, leading to its regression (Mancini et al., 2021). Following the restoration of the natural

environmental conditions after the end of the wreck removal operation (July 2014) and the seabed cleaning phase (April 2018), transplanting operations of *P. oceanica* fragments started (2019) within the site. Nowadays, the area displays a complex mosaic of habitats, including hard rocky substrates (granitic rocks in the form of boulders and pebbles covered by a dense carpet of photophilic algae), soft (sandy and dead

'matte' substrates) as well as natural (high-density meadow) and transplanted (low-density meadow) *P. oceanica* beds.

The sea temperature was monitored daily using four HOBO Onset data loggers (Logger UA-002-64) positioned inside the study area at 10, 15, 20 and 30 m depth.

### 2.3. Underwater imagery collection

Photogrammetric image acquisition was conducted bimonthly from January 2022 to November 2022, following the protocol successfully applied to monitor *Posidonia* transplantation progress (Ventura et al., 2022). To ensure correct georeferencing, scaling, and overlap between the final cartographic products, including Digital Surface Models (DSMs) and orthophoto mosaics, 11 Ground Control Points (GCPs) were identified within the study area. The GCPs coordinates and depth measurements were accurately derived using two low-cost single-frequency (L1-1575.42 MHz) Global Navigation Satellite System (GNSS) receivers (Emlid Reach RS + units, <https://emlid.com/reachrs/>), working in real-time kinematic positioning mode. The base unit was installed on a known trig point on the coast, ensuring a short baseline (<1.5 km). The rover unit was mounted on a rigid marker buoy manoeuvred by a snorkelling operator from the surface. GCPs consisted of conspicuous structures on the seabed, easily recognizable in the acquired images, such as the vertices of 1 m<sup>3</sup> concrete clump weights. The underwater operator was equipped with a diver propulsion vehicle (DPV) to optimize image collection and allow the imagery acquisition on a large scale. The DPV vehicle was equipped with a spirit level, compass, and depth gauge, ensuring a constant navigation path, a fundamental step for achieving correct image overlap and subsequent camera alignment and mosaicking. A GoPro Hero 10 Black Edition action camera was installed with its underwater housing below the DPV, pointing at a near-nadir position. Images were acquired every 2 s along transects spaced no more than 4 m, ensuring an image footprint of approximately 65 m<sup>2</sup> with a ground sample distance of 2–3 mm/pixel (Table 1). The mapping effort was limited to a depth of 25 m due to safety constraints linked to the permanence of the diver underwater and because of the limited presence of natural light that posed a significant challenge for capturing underwater photographs when external lighting equipment, such as strobes and flashes, was not utilized.

### 2.4. Underwater imagery processing

Imagery processing was performed on an ASUS ROG G703 workstation (Intel core i7-7700HQ CPU, 48 GB RAM, Nvidia Geforce GTX1080 graphic card) running Agisoft Metashape v. 1.8.2. (Agisoft LLC, Russia), a low-cost platform for 3D reconstructions using SfM algorithms. Sparse point clouds were obtained by aligning digital images derived from each mapping mission (Table 1 supplementary materials). Subsequently, sparse point clouds were enhanced by Multi-View Stereo algorithms, resulting in dense point clouds. Following the manual detection of GCPs, each point cloud was scaled to real-world XYZ coordinates by adding GNSS coordinates to each GCP. A subset of the surveyed GCPs was excluded from the photogrammetric processing within the SfM workflow, specifically during the bundle adjustment

phase. This exclusion occurred because five were designated as validation points, or checkpoints (CPs), and utilized to evaluate the positional accuracies obtained following the bundle adjustment. Using CPs offers a more objective assessment of the accuracy of georeferencing methods compared to evaluations based solely on GCPs (Ferrer-González et al., 2020). Therefore, CPs were identified in the orthoimages, and their coordinates were compared to the surveyed GNSS positions. The overall registration accuracy at each CPs was evaluated by the root mean square error (RMSE) of the GNSS coordinate residuals and the spatial errors in easting (X), northing (Y), depth (-Z) directions, and in the 3D space (XYZ). Low RMSE values signify effective image alignment and block adjustments, leading to accurate georeferenced products. The dense point cloud data were ultimately subjected to interpolation through the Inverse Distance Weighting method, facilitating the creation of DSMs employed in the orthorectification process and the assembly of image mosaics.

### 2.5. GIS analysis for habitat mapping

At each sampling event, approximately 6500 m<sup>2</sup> were effectively mapped; however, a smaller region of interest (ROI), defined using a polygon mask that encompassed 5500 m<sup>2</sup>, was used for the following analysis in a geographic information systems (GIS) environment. This approach was adopted to exclude marginal areas that could be influenced by poor geometries and inaccuracies resulting from minimal image overlap. After masking the ROI, the orthophoto mosaics and DSMs in GeoTIFF format were analyzed in ESRI® ArcMap v. 10.6. using the Benthic Terrain Modeller tool (De Oliveira et al., 2020) to derive seabed terrain metrics such as slope, rugosity, and vector ruggedness measure (VRM) using the surface properties of the raster cells in 3 × 3 cm window. The zonal statistics tool was then employed to extract mean values for the above-mentioned seabed metrics utilizing a superimposed regular grid with a cell size of 1 m × 1 m. The chosen grid size was deemed adequate for describing the habitat used by the species, given that sea cucumbers exhibit notable site fidelity and a relatively limited home range. This is consistent with findings related to other species, which typically exhibit daily movement distances ranging from 2 to 9 m (Siegenthaler et al., 2015; Wolfe and Byrne, 2017). Every visible sea cucumber inside the ROI was manually digitized as a polygon in the orthophoto mosaics to estimate holothurian abundances for each sampling event. Body length in cm, depth in m, degree of debris coverage (recorded in three classes: <30%, 30–60%, and >60%), and re-projected coordinates of the shape centroid measured as Easting and Northing (UTM-WGS84, zone 32 N, EPSG: 32,632) were collected for each individual. Due to the very high spatial resolution of the images, an object image analyses (OBIA) approach was adopted to speed up the orthophoto mosaic classification and derive benthic habitat cover classes (Fallati et al., 2023). The methodology involved two main steps: applying segmentation algorithms to group pixels into homogenous regions (segments) based on spectral and geometric characteristics and, thus, classifying them into specified classes. Ortho-rectified photo mosaics were imported into the eCognition Developer 10 (Trimble, Sunnyvale, California, USA) software to perform OBIA. After band normalization, before the development of the OBIA ruleset, the

**Table 1**

Camera specifications and primary settings utilized for capturing underwater images with the Diver Propulsion Vehicle (DPV).

| Camera specifics   |                     | Camera settings             | Diver Propulsion Vehicle (DPV) |                              |                           |
|--------------------|---------------------|-----------------------------|--------------------------------|------------------------------|---------------------------|
| Camera model       | GoPro Hero 10 Black | EV Compensation             | –0.5                           | DPV model                    | Seacraft Future 1000      |
| Weight             | 156 g               | Shutter Interval            | 2.0 s                          | Steering mode                | Two-hand                  |
| Sensor type        | CMOS Sony IMX677    | White Balance               | Native                         | Gear dynamics (acceleration) | Slow                      |
| Sensors size       | 1/2.3", 23.6 MP     | ISO range                   | 100–800                        | DPV Speed                    | 25 m/min (~0.5 m/s)       |
| Sensors dimensions | 6.17 × 4.55 mm      | Time-lapse interval time    | 2 s                            | GSD (ground sample distance) | ~2 mm/px                  |
| Focal length       | 2.71 mm             | Frontal Overlap             | 85%                            | Distance from the seabed     | 4–5 m                     |
| Aperture           | f/2.5               | Lateral Overlap             | 75%                            | Mean (±SD) diving time       | 76 ± 7 min                |
| Image size         | 5568 X 4176         | Mean (±SD) number of images | 2076 ± 275                     | Mean (±SD) covered area      | 6500 ± 260 m <sup>2</sup> |

complexity of the data was initially reduced by using both a convolution (with Gauss Blur formula to remove noise) and a median filter (with a kernel size of 5) on the original red (R), green (G), and blue (B) bands. A multi-resolution segmentation (scale parameter = 60, shape = 0.5, compactness = 0.5) was adopted to group pixels into homogeneous regions (objects) based on their spectral differences due to red-green-blue bands while considering as attributes in the segmentation process elevation data derived from DSM, slope, rugosity, and VRM. After the segmentation process, a supervised classification technique was used to classify the imagery into the five main cover classes: i) sandy bottoms, ii) hard bottoms covered by photophilic algae, iii) dead ‘matte’ of *P. oceanica*, iv) natural *P. oceanica* meadow, and v) transplanted *P. oceanica*. At least 40 well-defined samples were selected for each class to serve as training areas for the classification algorithm. The support vector machine algorithm was used to classify the segments, considering all information derived from the input dataset, such as spectral value, brightness, size, and shape. After the classification, the adjacent segments were merged, and the final output was exported as a shapefile. A global accuracy evaluation was performed using a point-based approach, incorporating 300 randomly selected points. The assessment of accurate class assignment was conducted visually by analyzing high spatial resolution imagery, creating a confusion matrix that quantitatively measures actual versus predicted seabed classes to examine overall, Kappa, User’s, and Producer’s accuracies.

### 3. Data analysis

The Kruskal-Wallis’s hypothesis test was applied to evaluate the differences in size classes-habitat variables in all analyses. In case of significant differences (p-value  $\leq 0.05$ ), Dunn’s post hoc pairwise comparisons test was applied to indicate which data groups differ. The seabed cover class ‘*P. oceanica* meadow’ was excluded from the analysis because the dense canopy formed by the seagrass prevents the extraction of sea cucumber abundance data from the acquired imagery.

Principal components analysis was employed to explore the potential pattern between the physical variables characterizing each grid cell exhibiting the presence (recorded as density = N. ind/m<sup>2</sup>) and absence of sea cucumbers.

#### 3.1. Modelling approach

The spatial distribution of the observed individuals was modeled as a realization of a Log-Gaussian Cox Process (LGCP) to examine how particular geomorphological characteristics and the variety of habitats found on the seabed influence the ecological dynamics of sea cucumber populations. In the context of the LGCP framework, the logarithm of the intensity function  $\log(\lambda)$  is represented as a Gaussian process, which renders it especially appropriate for environmental and ecological datasets that demonstrate spatial dependence with some aggregation or clustering behaviour (Williamson et al., 2022). Inhomogeneous Poisson point processes can also be employed to fit simple point process regression models to data; however, this approach relies on an independence assumption among point events, which may impose significant limitations. Alternatively, LGCP are frequently utilized, as they incorporate a latent Gaussian random field into the model. This addition allows for the representation of further clustering among point events that extends beyond the explanatory capacity of a Poisson model (Dovers et al., 2024). A spatio-temporal model was used to consider multiple sampling campaigns throughout 2022. The recorded positions, i.e., defined by their spatial ( $s \in D \subset \mathbb{R}^2$ ) and temporal ( $t = 1, \dots, T$ ) locations of sea cucumbers, was treated as a point process. This process allowed for the intensity function  $\lambda(s, t)$  to be modeled based on various predictors, such that:

$$\log(\lambda(s, t)) = \beta_t + X(s)\beta + w(s) \quad (\text{Eq. 1})$$

Here  $\beta_t$  was a temporal intercept,  $X(s)$  was a set of spatial covariates that are time-independent,  $\beta$  was the vector of the linear effects related to the spatial covariates. Finally,  $w(s)$  was a zero-mean Gaussian process with a Matérn spatial covariance function. A Matérn covariance of order 1 with range  $\rho$  and standard deviation  $\sigma$  (Martino et al., 2021; Yuan et al., 2017) was adopted. The spatial covariates were stored as a regular grid of 1 m  $\times$  1 m cell size. The mean values of the cells were associated with the centroid points, and the values of the other points  $s \in D$  were interpolated using Inverse Distance Weighting. The following covariates were included: slope, depth, rugosity, temperature, VRM, and habitat classification. The correlation among the predictors was assessed, leading to the exclusion of rugosity and temperature from our model. Consequently, only the variables VRM and the y-coordinate were retained to avoid multicollinearity. For the parameters of the spatial field  $w(s)$  in (1), the PC priors method (Fuglstad et al., 2019) with setting  $P(\rho < 100) = 0.5$  and  $P(\sigma > 0.7) = 0.01$  was used. For each  $\beta_t$  an independent non-informative improper flat prior was adopted, while Gaussian priors with mean 0.0 and precision 0.001 were independently assigned to each component of  $\beta$ . The results were obtained using scaled spatial covariates between 0 and 1 to standardize them and avoid scale effects. The SPDE approach (Simpson et al., 2016) based on the results of (Lindgren et al., 2011) was followed. The rationale was to approximate the Gaussian process with Matérn covariance with a finite representation, which allowed to rewrite the hierarchical model as the Gaussian Latent Model (GLM) with Poisson Likelihood, which can be used in *inlabru* and *INLA*.

### 4. Results

#### 4.1. High spatial resolution habitat mapping

The entire ROI of 5500 m<sup>2</sup> was systematically mapped in every sampling occasion (February, April, June, August, and October) by a single dive with a mean duration of 76 min  $\pm$  7 min that allowed the acquisition of 1800–2500 underwater digital photos, displaying a mean image footprint overlap from 3 up to 45 images (Table 2 Supplementary materials). Approximately 16 h were required to generate the main SfM outputs in Agisoft Metashape, encompassing the detection of GCPs for producing georeferenced sparse and dense point clouds with an average point density of 12,456  $\pm$  1315 points/m<sup>2</sup>, DSMs, and high spatial resolution (1.2–1.8 mm/pixel) orthophoto mosaics (Fig. 2a–d). After bundle adjustment transformations, the spatial accuracy of the photogrammetric model measured at CPs resulted in an RMSE of 9.3, 17.7, and 26.6 cm in easting, northing, and vertical (depth) components, respectively (Table 3 Supplementary materials). The GIS analysis of DSMs and orthophoto mosaics allowed the creation of other informative raster layers representing the slope (observed range from 0° on flat sandy areas to 90° on vertical hard bottoms and artificial structures), the VRM (observed range from 0 on homogeneous sandy areas to 0.82 on complex hard bottoms, artificial structures, and *Posidonia* canopy), and the five cover classes identified after OBIA (Fig. 3a–d). Sandy bottoms represented the most common class with a cover of 52.3%, followed by

**Table 2**

Total number of sea cucumbers (N), mean density of individuals (Ind./m<sup>2</sup>), mean, minimum and maximum length estimated for the five sampling occasions in 2022 through manual detection and count inside 1  $\times$  1 m cell grid over imposed on Structure from Motion (SfM) orthophoto mosaics.

| Sampling month | N    | Ind./m <sup>2</sup> $\pm$ SD | Mean length (cm) $\pm$ SD | Min length | Max length |
|----------------|------|------------------------------|---------------------------|------------|------------|
| February       | 984  | 1.18 $\pm$ 0.45              | 26.56 $\pm$ 5.55          | 10.67      | 50.07      |
| April          | 1479 | 1.24 $\pm$ 0.52              | 25.9 $\pm$ 5.47           | 8.7        | 46.21      |
| June           | 938  | 1.19 $\pm$ 0.47              | 24.57 $\pm$ 5.19          | 9.94       | 41.97      |
| August         | 770  | 1.16 $\pm$ 0.42              | 25.73 $\pm$ 4.91          | 12.08      | 47.19      |
| October        | 668  | 1.14 $\pm$ 0.4               | 23.31 $\pm$ 5.54          | 9.33       | 48.05      |

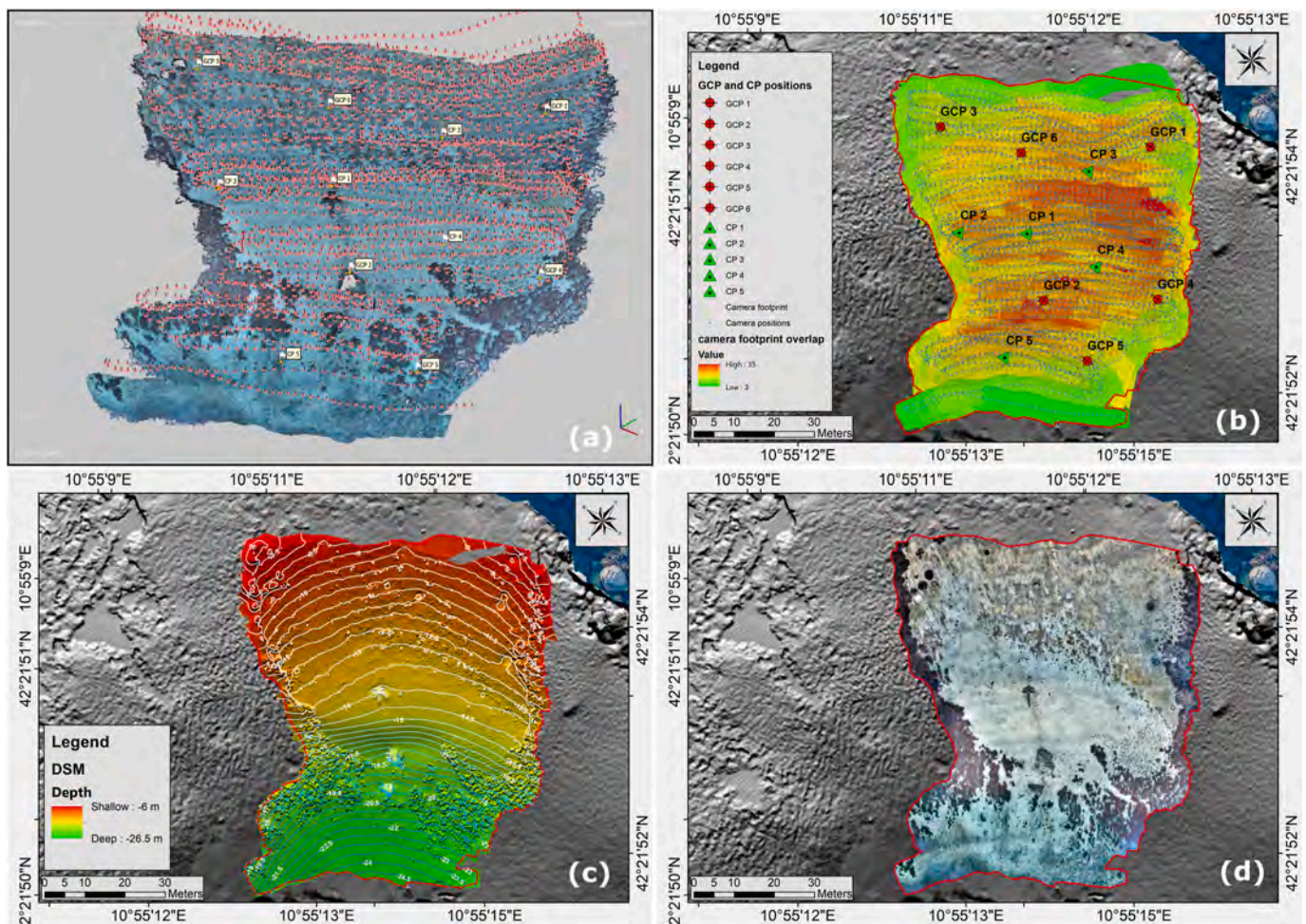


**Fig. 2.** The main outputs obtained from the Structure from Motion (SfM) processing of underwater imagery following the first mapping campaign conducted in February 2022. a) The georeferenced dense point cloud; b) Geolocalization of ground control points (GCPs) and checkpoints (CPs) with estimated camera positions (small blue dots) and image footprint overlap; c) the digital surface model represented by colour-hillshade relief with depth contour at 0.5 m intervals; d) the high spatial resolution orthophoto mosaic of the study area.

*Posidonia* meadow (19.6%), dead ‘matte’ (17.6%), hard bottoms (8.9%) and transplanted *Posidonia* (1.6%). OBIA segmentation and classification showed high performance in terms of overall accuracies (87.3%) and Kappa coefficients (83%), providing adequate identifications of the five cover classes. Significant misclassification errors were observed between the cover classes of ‘matte’ and ‘hard bottoms’ attributed to the existence of comparable photophilic algal communities that produce analogous spectral signatures (Fig. 1 and Table 4 in the Supplementary materials).

#### 4.2. Sea cucumbers population dynamics and habitat preferences

The underwater visual census carried out by SCUBA divers reported that the sea cucumber population in the area was mainly constituted by *Holothuria tubulosa*, representing 92% of the benthic assemblages, followed by *H. poli* (6%) and *H. mammata* (2%). A total of 4839 sea cucumbers were identified through manual detection and count on SfM-based orthophoto mosaics. These organisms exhibited a consistent presence throughout the year across the entire bathymetric range with similar densities (Table 2), with peaks in abundance occurring in February (N = 984) and April (N = 1479).

Length-frequency distributions showed that a more significant proportion of individuals from larger size classes were observed during these months compared to other sampling events (Fig. 4a). A bathymetric distribution was reported since smaller individuals were more

commonly found in shallow water areas (10–15 m), whereas larger size classes were observed at greater depths (Fig. 4b). Detritus cover percentage significantly differed according to the length of sea cucumbers with more substantial differences reported among specimens belonging to small and medium-sized length classes, especially when thriving in deeper areas (Fig. 5c).

The grid cells that exhibited the presence of at least one sea cucumber, with a maximum of five specimens per square meter, showed a consistent proportion (>60%) of sand. This preference for sand decreased as the size of the individuals diminished. Small and medium-sized sea cucumbers were also observed in cells with high cover percentages of various substrates, including dead ‘matte’, hard bottoms (predominantly pebbly areas covered by algal mats) and transplanted *P. oceanica* fragments (Fig. 5a). An increasing trend in the utilization of both sloping and higher terrain complexity areas was observed moving from large to small size classes due to their association with more complex habitats such as pebbly patches and transplanted *P. oceanica* seedlings (Fig. 5b and c).

The first three axes from principal components biplots (Fig. 6) explained approximately 61.3% of the information, corroborating the hypothesis of an active selection for specific seabed cover classes. The analysis also highlighted a negative association between holothurian density (Ind./m<sup>2</sup>) and severe sloping areas (>20°) with large terrain ruggedness (VRM >0.5) values. In particular, the first dimension (Dim 1) represented 25.4% of the variation and loaded mostly for sandy flat

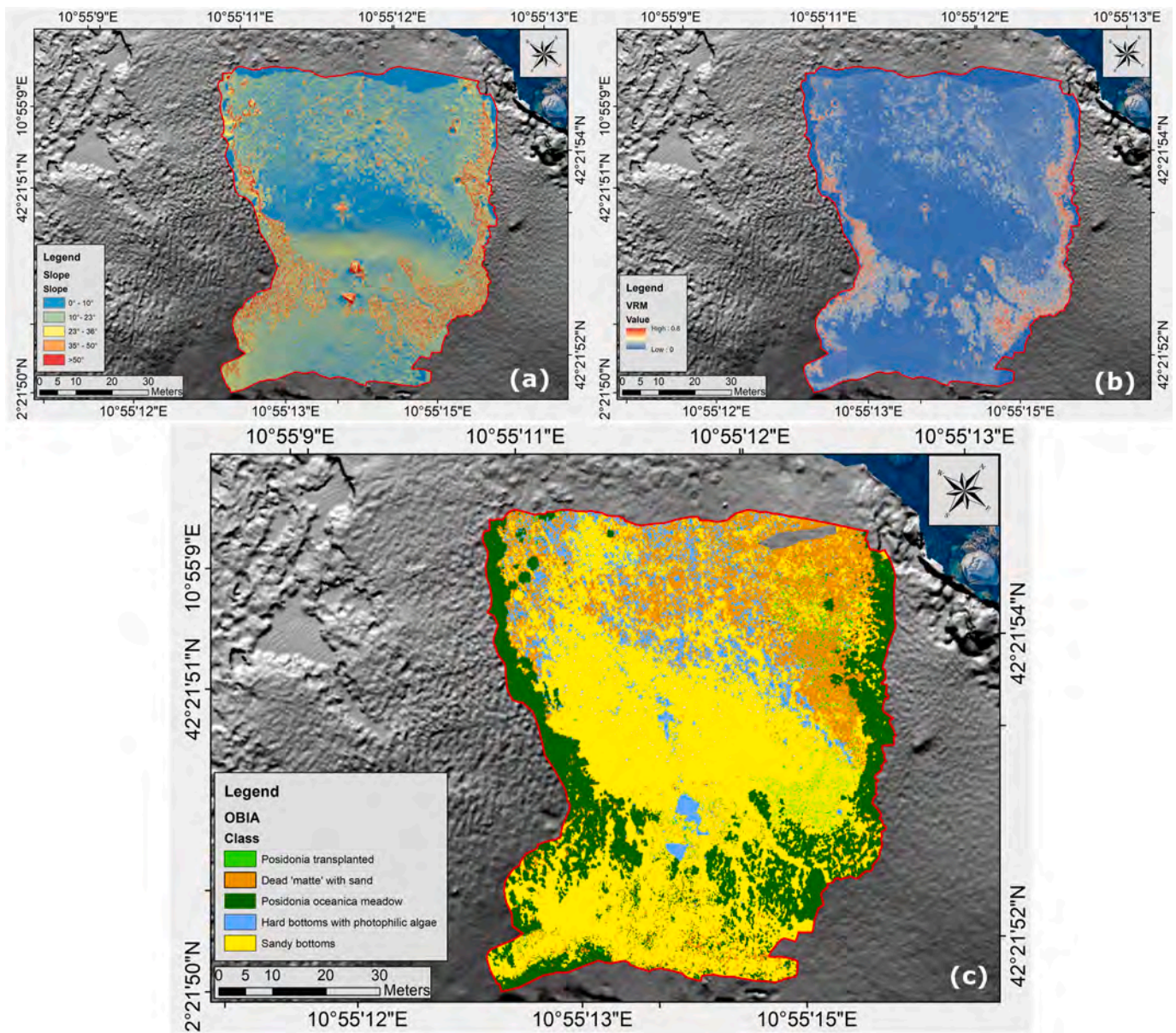


**Fig. 3.** Additional raster layers derived after GIS analysis of the main SfM products (digital surface model and orthophoto mosaic). a) Seabed slope; b) Seabed vector ruggedness measure (VRM); c) Thematic map with five seabed cover classes (transplanted *Posidonia oceanica* fragments, dead 'matte' of *P. oceanica*, *P. oceanica* meadow, hard bottoms covered by photophilic algae, and sandy bottoms) generated after image segmentation and classification during OBIA workflow.

(slope  $<10^\circ$ ) habitats extending in intermediate and deep-water areas, characterized by low VRM values (0–0.15). The second (Dim 2) and third (Dim 3) dimensions explained 23.2% and 12.7% of the variation, respectively, with strong loadings for shallow areas with moderate VRM values (up to 0.25) such as those covered by dead 'matte' or transplanted fragments of *P. oceanica* (Fig. 7). The temperature exhibited an inverse correlation with depth, attributed to the significant presence of a shallow thermocline during the summer months (Fig. 2 supplementary material).

#### 4.3. Sea cucumbers' spatial and temporal patterns

The mean log-intensity  $\log(\lambda(s))$  of the LGCP model fitted on the sea cucumber occurrence locations demonstrates a non-random spatial pattern for the five sampling occasions. During cold months (February and April), sea cucumbers were widely distributed across the study area, spanning from shallow to more deep habitats. Conversely, during the summer and autumn months, an evident shrinking of the spatial distri-

butions was detected, with the highest intensity values reported only inside the *P. oceanica* transplantation area (Fig. 7a and b-c-d-e). In fact, the portion of the study area contoured by the 90th–100th percentile interval of the log-intensity distribution varied from 1546 m<sup>2</sup> in April to a minimum of only 94 m<sup>2</sup> in October, highlighting a concentration of individuals in the seagrass transplantation area after the summer (Fig. 7f). The central region, distinguished by a sandy patch with a slope exceeding 15°, consistently exhibited the lowest intensity values. The estimated fixed effects derived from the model demonstrated that all temporal and habitat variables significantly impacted the mean log intensity, suggesting that the spatial distribution of individuals varied according to the month and the characteristics of the sea bottom. In contrast, within the geomorphological factors, only the variables associated with slope and VRM negatively impacted the mean intensity of the sea cucumber population, with the latter factor contributing more significantly (Fig. 8).

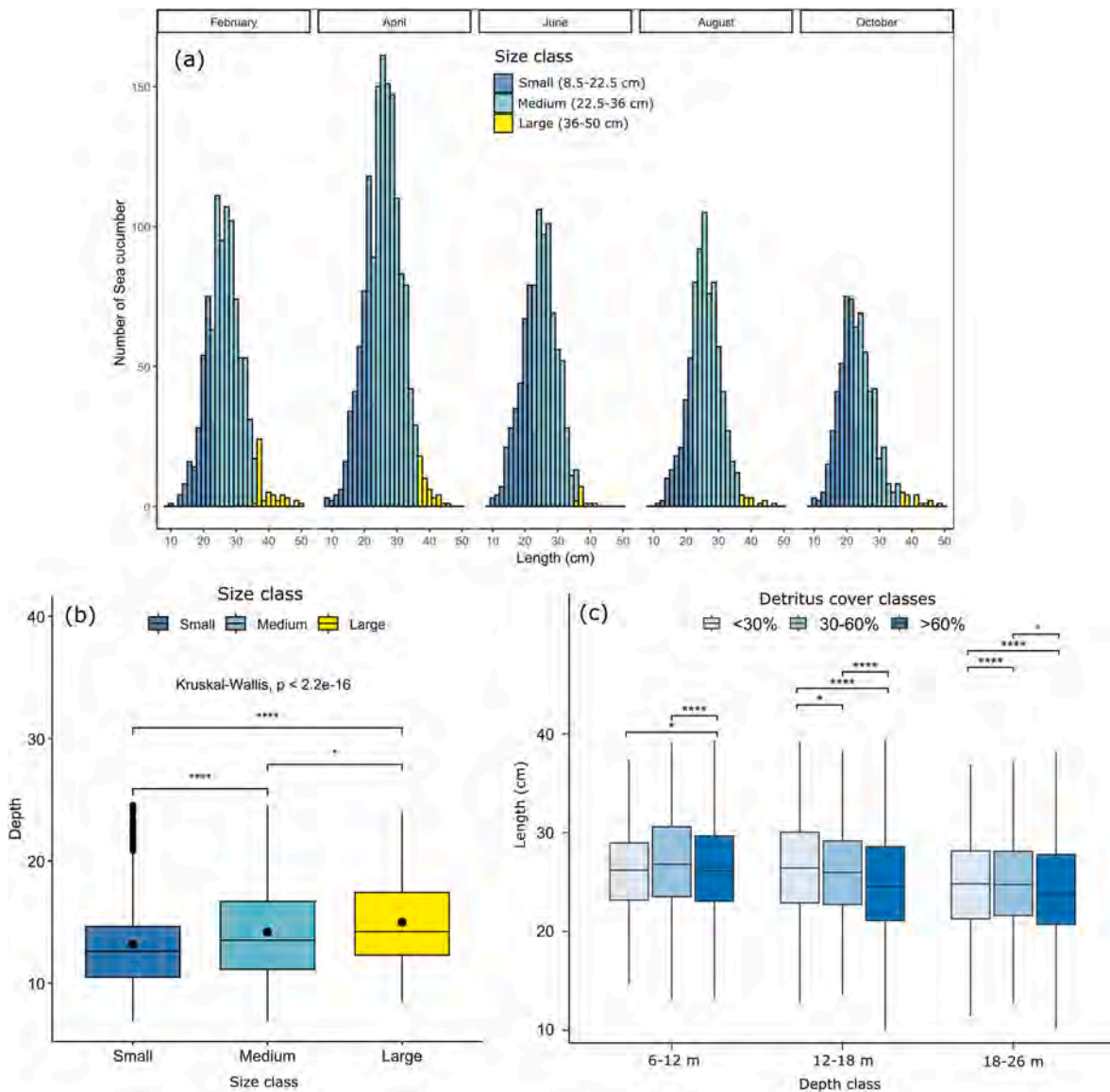


Fig. 4. a) Length-frequency distribution of the three size classes recorded in the study area from February to October 2022. Boxplots reporting sea cucumber size class distribution according to depth (b) and (c) the degree of detritus cover along the three depth classes (shallow: 6–12 m, intermediate: 12–18 m and deep: 18–25 m). Significance codes: \*\*\* $p < 0.001$ ; \*\* $p < 0.01$ ; \* $p < 0.05$ ; ns = non-significant.

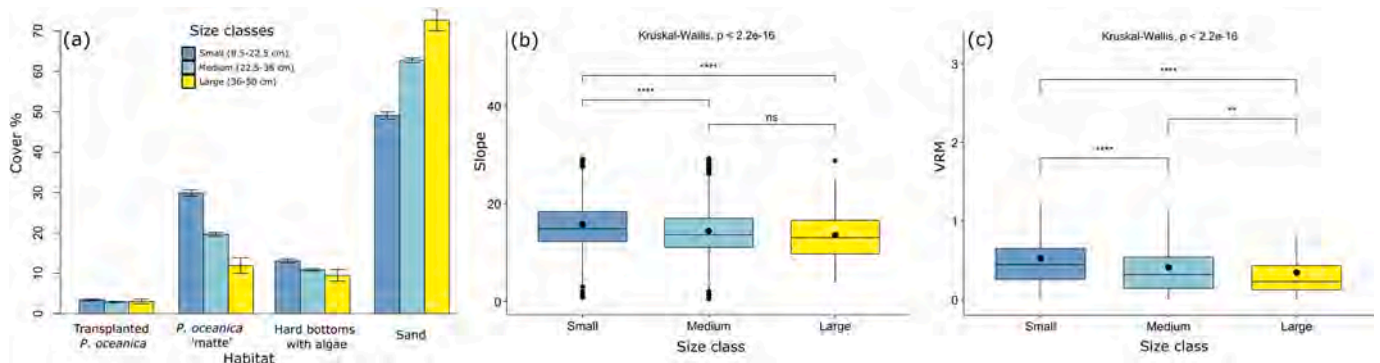
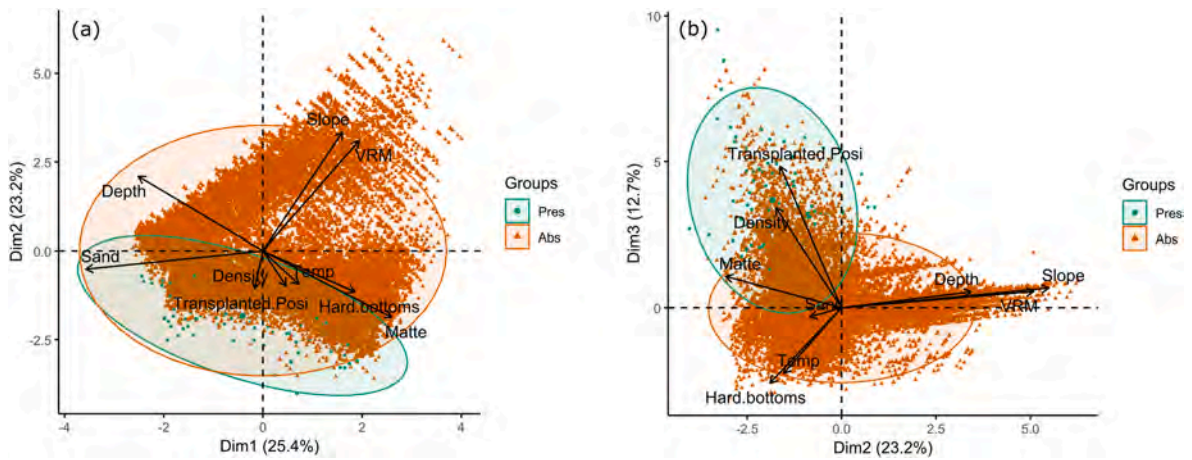
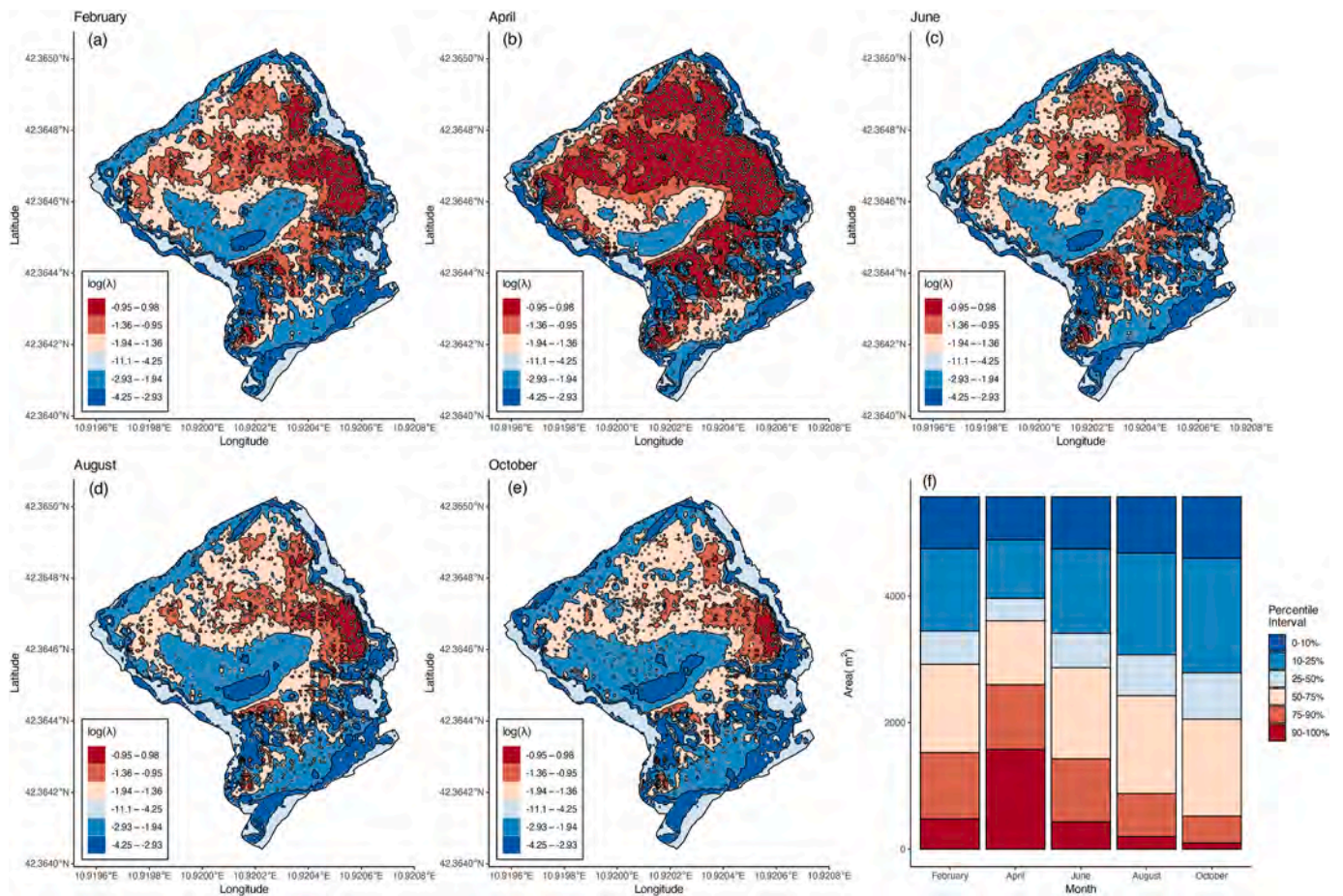


Fig. 5. Sea cucumber habitat use expressed as (a) mean cover percentage of the four categories of the seabed classes, (b) mean slope, and (c) mean vector ruggedness measure (VRM) recorded for each 1 x 1-m grid cell that contains at least one specimen. Significance codes: \*\*\* $p < 0.001$ ; \*\* $p < 0.01$ ; \* $p < 0.05$ ; ns = non-significant.



**Fig. 6.** Principal component analysis (PCA) biplots reporting loadings on the dimensions 1–2 (a) and 2–3 (b) based on sea cucumber density assessed within 1 × 1m grid cells. This analysis includes seven habitat variables, consisting of the four categories of seabed cover and variables related to terrain ruggedness (VRM), depth, slope and sea temperature.



**Fig. 7.** Predicted posterior log intensity  $\log(\lambda(s))$  of sea cucumbers in the study area after Log-Gaussian Cox Process (LGCP) modelling (a-b-c-d-e): Spatial and temporal patterns were reported during the five sampling occasions. The colour ramp from red to blue indicates high and low intensity, respectively. (f) The surface area is enclosed within different percentile intervals of the log-intensity distribution in the five sampling occasions. The colours match the other panels of the figure.

**5. Discussion**

Fine-scale environmental metrics, including slope, rugosity, and habitat type, play a pivotal role in the dynamics of sea cucumber communities. These factors must be meticulously considered when analysing broader ecological data obtained through extensive methodologies that

may lack resolution, such as traditional fishery-based approaches. At the same time, research focused on delineating the ecological requirements of sea cucumbers is equally essential for understanding potential policy implications for resource managers who must navigate the challenge of reconciling the socio-economic impacts on ecosystem productivity and diversity with the socio-economic pressures faced by fishers seeking to

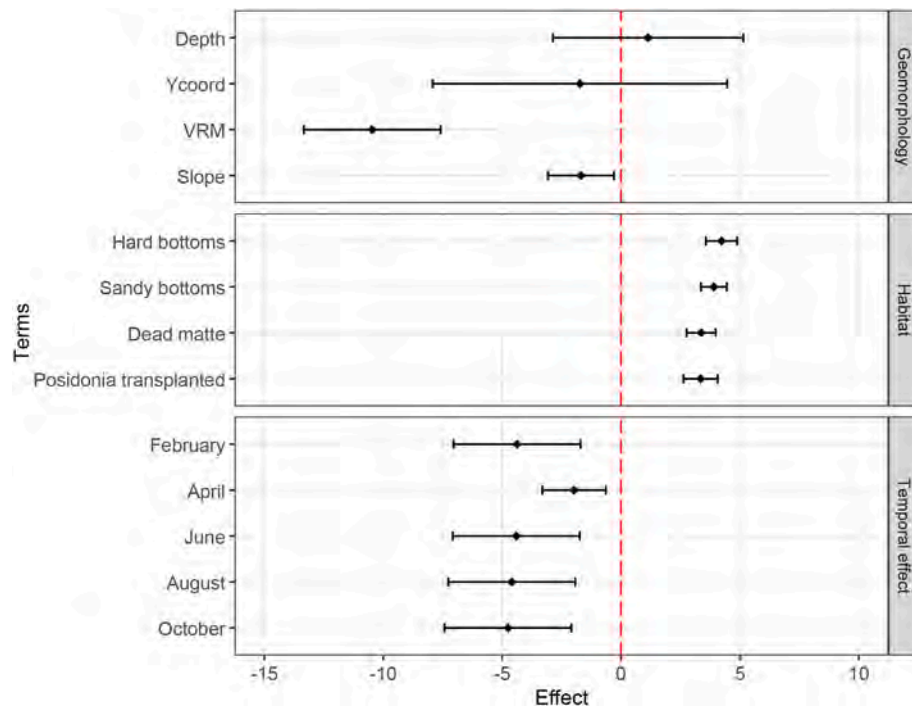


**Fig. 8.** Forest plot of the estimated fixed effects and 95% credibility intervals related to the different terms retained in the final Log-Gaussian Cox Process (LGCP) model, capable of influencing sea cucumber log-intensity  $\log(\lambda(s))$  in the study area. Remember that if the line crosses the zero reference, the effect is non-significant.

exploit this resource (Purcell et al., 2016a). Recognizing the ecological functions of harvested species and understanding the possible consequences of their removal on the ecosystem's functionality are pivotal issues in ecosystem-based fisheries management, which seeks to maintain robust marine ecosystems and the fisheries that depend on them (Hilborn, 2011). The growing demand in Asian markets has resulted in the swift development of new fisheries across different areas, particularly in the Mediterranean, where the main commercially targeted species belong to the genera *Holothuria* and *Parastichopus* (Neofitou et al., 2019). *Holothuria tubulosa* is among the most exploited Mediterranean species, with extensive Illegal, Unreported and Unregulated fishery among several Mediterranean countries (Rakaj and Fianchini, 2024). Its heavy exploitation as bait for long-line fisheries has led to a notable decrease in harvested population, especially in the southern Aegean Sea (Kazanidis et al., 2010). Moreover, in recent years, significant commercial interest in employing Mediterranean sea cucumbers as extractive species for waste mitigation in integrated multi-trophic aquaculture systems (Grosso et al., 2021) deserves specific attention, especially considering that overexploitation of this species can trigger cascading effects on ecosystems (Price et al., 2010). Unfortunately, the management strategies to ensure a sustainable fishery for this target resource remain limited or lacking in many Mediterranean regions (Rakaj et al., 2018). To our knowledge, no prior studies have identified, at comparable scales and accuracy, specific microhabitat requirements for temperate sea cucumbers, particularly for *H. tubulosa*, which is one of the most common species on the Mediterranean coast.

In this context, the methodology presented offers an innovative remote sensing approach for quantifying the sea cucumber population and evaluating their habitat preferences across complex coastal areas. The mapping method used could easily be employed for high-value commercial species where they occur in shallow reefs or intertidal lagoons (Hammond et al., 2020), filling the gaps in counts made by both drone imagery and snorkeler-based transects (Williamson et al., 2021) especially if integrated with recent deep learning algorithms used for automatic detection (Li et al., 2021). However, in these recent applications, the extent of the surveyed area is still limited to very shallow coastal areas such as coral reef flats exposed during low tide, making

them unsuitable for Mediterranean infralittoral species. The requirement for sufficient spatial resolution in the captured images to facilitate the detection of sea cucumbers necessitates low-altitude mapping missions, which, coupled with UAV battery duration, lead to limited spatial coverage. In addition, UAV-generated photomosaics can also be influenced by water refraction and turbidity, which may impede the detection of smaller or generally less conspicuous organisms. At the same time, SCUBA diver and snorkeler-based censuses, aside from the nature of the sampling method (e.g. point counts, strip transects, line transects, rapid visual counts), can be influenced by the experience of the personnel involved other than suffering of high logistics costs.

The results demonstrate the capability of SfM in discerning fine-scale ecological drivers, such as seabed complexity at a centimetre scale, which can significantly affect the distribution and abundance of sea cucumbers. Several studies have demonstrated that fine-scale structural complexity (expressed by geomorphological variables, such as VRM, DSM, slope, and aspect) plays a crucial role in shaping the biodiversity and abundance of fish assemblages (Borland et al., 2021; Levin et al., 2014), reef systems (Fukunaga et al., 2020) and macroinvertebrate communities (Hauser et al., 2006). However, its impact on benthic species seems to be considerable only until a specific threshold is reached, after which structural complexity's influence on species distribution becomes smaller (Lapointe and Bourget, 1999; Price et al., 2019) or even a limiting factor (Graham and Nash, 2013). In this study, VRM can be most likely associated with the density of *P. oceanica* shoots other than hard bottoms with simple morphologies such as pebbles and small rocks covered by photophilic algae. These findings indicated that the observed terrain ruggedness was associated with low to moderate values of VRM (ranging from 0.15 to 0.25), indicative of the *Posidonia* transplantation zones with low shoot densities (15–30 shoots/m<sup>2</sup>). These conditions appeared to favour the presence of sea cucumbers during the summer months. However, when VRM values exceed a certain threshold (0.3–0.5), the increased structural complexity acted as a limiting factor. Similarly, the relationship between the slope and the proportion of hard substrates can inhibit the movement of sea cucumbers, as the three-dimensional structure create grades. Consequently, sea cucumbers, especially large-size classes, preferred deeper flat (<10°)

sandy areas surrounded by seagrass meadows for foraging activities. This result, emerging for the first time through the SfM photogrammetric processing, perfectly aligns with the trophic behaviour of the genus *Holothuria*, which is described as an epi-benthic deposit feeder preferentially ingesting organic detritus from the water-sediment interface among soft bottoms with low hydrodynamic forces where organic matter can accumulate (Boncagni et al., 2019). In fact, the presence of open sand or sand characterized by 'ripple marks', considered a proxy of wave energy, was considered a factor capable of restricting holothuroid distribution (Massin and Doumen, 1986; Shiell and Knott, 2010). It should be noted that increasing VRM values or topographic heterogeneity is also indicative of greater surface area (Atrill et al., 2000), resulting in a more significant availability of shelters and diversity in hydrodynamic regimes patterns acting at the microscale (Bargain et al., 2018). This aspect can sensibly influence small-sized *H. tubulosa* specimens that were often reported in pebbly areas or near hard artificial structures capable of providing additional shelters. A comparable pattern was noted among small individuals of *H. mammata*, which displayed a fragmented distribution. Their habitat preferences were shaped by the availability of shelter, food resources, and the complexity of the habitat. In contrast, larger size classes demonstrated a greater tendency to opportunistically investigate less stable and more open sandy environments (Félix et al., 2024). The observed differential cover percentage of detritus among the censused individuals corroborated that smaller-sized classes are generally tended to be less conspicuous due to the accumulation of organogenic detritus, including shell fragments and their bodies. This phenomenon is particularly evident in deeper habitats, where larger fish may elevate predation risks for these smaller organisms (Francour, 1997).

Even if the microhabitats formed under transplanted *P. oceanica* fragments were not perfectly captured in DSMs, as they were rendered using a planar graphical projection from an elevated 'bird's-eye view', it is reasonable to think that the aggregation pattern observed denoted a strong preference for discontinuity zones formed by transplanted fragments of *P. oceanica* between sandy or dead 'matte' patches. These areas could serve as effective sinks for food sources, such as fine organic particles and phanerogamic detritus (Boncagni et al., 2019; Slater and Chen, 2015). These elements might be particularly crucial during the spawning season of *H. tubulosa*, which occurs in late August (Pasquini et al., 2022). This timing coincides with the observed high concentration of individuals near the transplantation area. In fact, like terrestrial plants, *P. oceanica* loses its leaves mainly in autumn and winter, and the rough sea conditions in these periods facilitate substantial accessibility to organic detritus across the whole area, thereby enhancing the dispersal of individuals. In contrast, during the summer, the transplanted *P. oceanica* seagrass meadows usually exhibited a greater quantity of brown senescent tissue compared to their natural counterparts (Bacci et al., 2024). This, along with the mortality of certain transplanted fragments and restricted water movement, resulted in a persistent accumulation of phanerogamic debris trapped among the rhizomes. Additionally, compared to more complex natural meadows, the transplanted meadows with a simpler habitat structure allowed for unhindered movement of sea cucumbers, thereby optimizing their foraging behaviour. Also, the geomorphological features of the area, predominantly shaped by southeast winds and currents, further contributed to the accumulation of organic matter, including that deriving from the adjacent natural meadows within the transplantation zone. All these factors may have influenced the observed distribution patterns in the transplantation area. As a result, we deduce that restored seagrass beds function as habitats for Mediterranean sea cucumbers species and, more importantly, as a food source by producing and retaining organic detritus. This detritus can be redistributed and altered beyond the transplantation zone due to the active bioturbation performed by these organisms (Boncagni et al., 2019; Neofitou et al., 2019).

The sea cucumber densities recorded in this study with a mean total value of  $118.2 \pm 0.03$  individuals/100 m<sup>2</sup> (considering the whole

bathymetric range investigated) can be regarded as relatively high when compared to Aegean Sea populations, exhibiting  $9.9 \pm 3.2$  individuals/100 m<sup>2</sup> (Kazanidis et al., 2010). On the other hand, for a dense *Posidonia* meadow, up to 377 individuals/100 m<sup>2</sup> were recorded from Ischia Island (Coulon and Jangoux, 1993), confirming that the density of *H. tubulosa* seems to be highly variable according to the availability of different habitat types and therefore require specific assessment to evaluate its preferences locally. However, the limitations in imagery-based acquisition made it unfeasible to assess the population of sea cucumbers in seagrass habitats characterized by dense vegetation, as the high density of shoots obstructed SfM reconstructions. Although such aspect can only be mitigated through *in situ* sampling or by using more invasive fishing gear (e.g., dredges), alternative configurations implying the use of advanced photographic equipment, such as professional full-frame cameras with larger pixel dimensions, can markedly improve image quality in comparison to consumer-grade action cameras. This enhancement in image quality may facilitate a more precise identification of species, leading to an improved evaluation of the size and composition of the population or stock. Lastly, it should be noted that the quantity and configuration of GCP can significantly influence the accuracy of a survey. Consequently, strategically placing a high density of precisely measured GCPs constitutes a critical component of the overall surveying process that should be carefully assessed when extensive areas must be mapped. In such circumstances, however, using acoustic-based data deriving from multibeam echo-sounders could provide a viable alternative for rough georeferencing of the acquired imagery, especially when conspicuous natural features can be well detectable from sonograms.

## 6. Conclusions

We provide a proof of concept demonstrating that SfM can yield new insights into localized habitat variables influencing sea cucumber population dynamics, which are essential for ecosystem functionality. For instance, the effectiveness of restoration efforts, often evaluated by including positive species interactions, should be carefully assessed in the context of sea cucumber removal for fishing purposes. Additionally, it could serve as a benchmark for comparing natural or protected population dynamics with those exploited by fishery, thereby facilitating an assessment of the impacts of fishing activities on these species.

The large-scale deployment of this protocol could contribute to developing tailored management strategies that are informed by a comprehensive understanding of the specific microhabitat requirements of benthic organisms by characterizing the sea cucumber stocks within a coastal region. Further investigations are required to overcome the constraints associated with imagery-based methods in dense natural seagrass meadows. Such investigations should focus on elucidating daily movement patterns and habitat utilization, as these elements could significantly influence the recycling of organic matter within seagrass ecosystems.

## CRedit authorship contribution statement

**Daniele Ventura:** Writing – review & editing, Writing – original draft, Visualization, Validation, Project administration, Funding acquisition, Formal analysis, Data curation, Conceptualization. **Arnold Rakaj:** Writing – original draft, Supervision, Data curation. **Giovanna Jona Lasinio:** Validation, Project administration, Data curation. **Gian Mario Sangiovanni:** Writing – review & editing, Software. **Daniele Poggio:** Writing – original draft, Validation, Formal analysis, Data curation. **Gianluca Mastrantonio:** Writing – original draft, Validation, Software, Formal analysis. **Alessio Pollice:** Visualization, Resources, Methodology, Formal analysis. **Gaia Grasso:** Methodology, Formal analysis, Data curation. **Edoardo Casoli:** Writing – original draft, Methodology, Data curation. **Gianluca Mancini:** Writing – original draft, Software. **Daniela Silvia Pace:** Writing – review & editing,

Writing – original draft. **Midhun Mohan**: Writing – review & editing, Writing – original draft, Validation. **Tommaso Valente**: Writing – review & editing, Writing – original draft, Supervision. **Andrea Belluscio**: Visualization, Validation. **Giandomenico Ardizzone**: Visualization, Validation, Supervision. **Stefano Moro**: Writing – review & editing, Writing – original draft, Visualization, Validation, Software, Formal analysis, Data curation.

### Declaration of competing interest

The authors declare the following financial interests/personal relationships which may be considered as potential competing interests: Daniele Ventura reports financial support was provided by DANIELE VENTURA. Daniele Ventura reports a relationship with DANIELE VENTURA that includes: funding grants. If there are other authors, they declare that they have no known competing financial interests or personal relationships that could have appeared to influence the work reported in this paper.

### Acknowledgements

This work was partially funded by the Pure Ocean Fund ('3DR-4-Seac' research grant) and PRIN 2002 (Project: LAGO-ON #number 20224LYJM5), which allowed the purchase of part of the equipment used during underwater in-field sampling. The involvement of D.P. in formal data analysis and presentation was made possible through the PNRR-NGEU project, which received financial support from the MUR (Ministry of University and Research) in accordance with DM 630/2024. We are indebted to two anonymous reviewers and editors for their valuable comments that have considerably improved the manuscript.

### Appendix A. Supplementary data

Supplementary data to this article can be found online at <https://doi.org/10.1016/j.jenvman.2025.124589>.

### Data availability

Data will be made available on request.

### References

- Attrill, M.J., Strong, J.A., Rowden, A.A., 2000. Are macroinvertebrate communities influenced by seagrass structural complexity? *Ecography* 23, 114–121.
- Azevedo e Silva, F., Brito, A.C., Pombo, A., Simões, T., Marques, T.A., Rocha, C., Madruga, A.S., Sousa, J., Venâncio, E., Félix, P.M., 2023. Spatiotemporal distribution patterns of the Sea Cucumber *Holothuria arguensis* on a rocky-reef coast (Northeast Atlantic). *Estuaries Coasts* 46, 1035–1045. <https://doi.org/10.1007/s12237-023-01201-1>.
- Bacci, T., Scardi, M., Tomasello, A., Valiante, L.M., Piazzini, L., Calvo, S., Badalamenti, F., Di Nuzzo, F., Raimondi, V., Assenzo, M., Cecchi, E., Penna, M., Bertasi, F., Piazzini, A., La Porta, B., 2024. Long-term response of *Posidonia oceanica* meadow restoration at the population and plant level: implications for management decisions. *Restor. Ecol.* e14360 <https://doi.org/10.1111/rec.14360>.
- Bargain, A., Fogliani, F., Pairaud, I., Bonaldo, D., Carniel, S., Angeletti, L., Taviani, M., Rochette, S., Fabri, M.-C., 2018. Predictive habitat modeling in two Mediterranean canyons including hydrodynamic variables. *Prog. Oceanogr.* 169, 151–168.
- Bayley, D.T.I., Mogg, A.O.M., 2020. A protocol for the large-scale analysis of reefs using Structure from Motion photogrammetry. *Methods Ecol. Evol.* 11, 1410–1420. <https://doi.org/10.1111/2041-210X.13476>.
- Boncagni, P., Rakaj, A., Fianchini, A., Vizzini, S., 2019. Preferential assimilation of seagrass detritus by two coexisting Mediterranean sea cucumbers: *Holothuria polii* and *Holothuria tubulosa*. *Estuar. Coast Shelf Sci.* 231, 106464. <https://doi.org/10.1016/j.ecss.2019.106464>.
- Borland, H.P., Gilby, B.L., Henderson, C.J., Leon, J.X., Schlacher, T.A., Connolly, R.M., Pittman, S.J., Sheaves, M., Olds, A.D., 2021. The influence of seafloor terrain on fish and fisheries: a global synthesis. *Fish Fish.* 22, 707–734.
- Burns, J.H.R., Delparte, D., Kapono, L., Belt, M., Gates, R.D., Takabayashi, M., 2016. Assessing the impact of acute disturbances on the structure and composition of a coral community using innovative 3D reconstruction techniques. *Methods Oceanogr.* 15–16, 49–59. <https://doi.org/10.1016/j.mio.2016.04.001>.
- Coulon, P., Jangoux, M., 1993. Feeding rate and sediment reworking by the holothuroid *Holothuria tubulosa* (Echinodermata) in a Mediterranean seagrass bed off Ischia Island, Italy. *Mar. Ecol. Prog. Ser.* 201–204.
- De Oliveira, N., Bastos, A.C., da Silva Quaresma, V., Vieira, F.V., 2020. The use of Benthic Terrain Modeler (BTM) in the characterization of continental shelf habitats. *Geo Mar. Lett.* 40, 1087–1097.
- Derehli, H., Aydin, M., 2021. Sea cucumber fishery in Turkey: management regulations and their efficiency. *Reg. Stud. Mar. Sci.* 41, 101551.
- Dovers, E., Stoklosa, J., Warton, D.I., 2024. Fitting log-Gaussian Cox processes using generalized additive model software. *Am. Statistician* 1–16.
- Fallati, L., Panieri, G., Savini, A., Varzi, A.G., Argentino, C., Büinz, S., 2023. Characterizing Håkon Mosby Mud Volcano (Barents Sea) Cold Seep Systems by Combining ROV-Based Acoustic Data and Underwater Photogrammetry.
- Félix, P.M., Azevedo e Silva, F., Simões, T., Pombo, A., Marques, T.A., Rocha, C., Sousa, J., Venâncio, E., Brito, A.C., 2024. Modelling the habitat preferences of the NE-Atlantic Sea cucumber *Holothuria forskali*: demographics and abundance. *Ecol. Inform.* 80. <https://doi.org/10.1016/j.ecoinf.2024.102476>.
- Ferrer-González, E., Agüera-Vega, F., Carvajal-Ramírez, F., Martínez-Carricondo, P., 2020. UAV photogrammetry accuracy assessment for corridor mapping based on the number and distribution of ground control points. *Remote Sens.* 12, 2447.
- Francour, P., 1997. Predation on holothurians: a literature review. *Invertebr. Biol.* 52–60.
- Fuglstad, G.-A., Simpson, D., Lindgren, F., Rue, H., 2019. Constructing priors that penalize the complexity of Gaussian random fields. *J. Am. Stat. Assoc.* 114, 445–452.
- Fukunaga, A., Burns, J.H.R., Pascoe, K.H., Kosaki, R.K., 2020. Associations between benthic cover and habitat complexity metrics obtained from 3D reconstruction of coral reefs at different resolutions. *Remote Sens.* 12, 1011. <https://doi.org/10.3390/rs12061011>.
- González-Wangüemert, M., Aydin, M., Conand, C., 2014. Assessment of sea cucumber populations from the Aegean Sea (Turkey): first insights to sustainable management of new fisheries. *Ocean Coast Manag.* 92, 87–94.
- Graham, N.A.J.J., Nash, K.L., 2013. The importance of structural complexity in coral reef ecosystems. *Coral Reefs* 32, 315–326. <https://doi.org/10.1007/s00338-012-0984-y>.
- Grosso, L., Rakaj, A., Fianchini, A., Morrioni, L., Cataudella, S., Scardi, M., 2021. Integrated Multi-Trophic Aquaculture (IMTA) system combining the sea urchin *Paracentrotus lividus*, as primary species, and the sea cucumber *Holothuria tubulosa* as extractive species. *Aquaculture* 534, 736268.
- Hamel, J.-F., Bondaroff, T.N.P., Mercier, A., 2024. Beyond beche-de-mer: sea cucumbers in nontraditional food products, health supplements, and biotechnology. In: *The World of Sea Cucumbers*. Elsevier, pp. 77–86.
- Hamel, J.-F., Eeckhaut, I., Conand, C., Sun, J., Caulier, G., Mercier, A., 2022. Global knowledge on the commercial sea cucumber *Holothuria scabra*. *Adv. Mar. Biol.* 91, 1–286.
- Hammond, A.R., Meyers, L., Purcell, S.W., 2020. Not so sluggish: movement and sediment turnover of the world's heaviest holothuroid, *Thelotrema anax*. *Mar. Biol.* 167, 1–9.
- Hauser, A., Attrill, M.J., Cotton, P.A., 2006. Effects of habitat complexity on the diversity and abundance of macrofauna colonising artificial kelp holdfasts. *Mar. Ecol. Prog. Ser.* 325, 93–100.
- Hilborn, R., 2011. Future directions in ecosystem based fisheries management: a personal perspective. *Fish. Res.* 108, 235–239.
- Kazaniadis, G., Antoniadou, C., Lolas, A.P., Neofitou, N., Vafidis, D., Chintiroglou, C., Neofitou, C., 2010. Population dynamics and reproduction of *Holothuria tubulosa* (Holothuroidea: Echinodermata) in the Aegean Sea. *J. Mar. Biol. Assoc. U. K.* 90, 895–901. <https://doi.org/10.1017/S0025315410000251>.
- Kilfoil, J.P., Rodriguez-Pinto, I., Kiszka, J.J., Heithaus, M.R., Zhang, Y., Roa, C.C., Ailloud, L.E., Campbell, M.D., Wirsing, A.J., 2020. Using unmanned aerial vehicles and machine learning to improve sea cucumber density estimation in shallow habitats. *ICES J. Mar. Sci.* 77, 2882–2889. <https://doi.org/10.1093/icesjms/fsaa161>.
- Lapointe, L., Bourget, E., 1999. Influence of substratum heterogeneity scales and complexity on a temperate epibenthic marine community. *Mar. Ecol. Prog. Ser.* 189, 159–170.
- Levin, P.S., Kelble, C.R., Shuford, R.L., Ainsworth, C., deRyner, Y., Dunsmore, R., Fogarty, M.J., Holsman, K., Howell, E.A., Monaco, M.E., 2014. Guidance for implementation of integrated ecosystem assessments: a US perspective. *ICES J. Mar. Sci.* 71, 1198–1204.
- Li, J.Y.Q., Duce, S., Joyce, K.E., Xiang, W., 2021. SeeCucumbers: using deep learning and drone imagery to detect sea cucumbers on coral reef flats. *Drones* 5, 1–19. <https://doi.org/10.3390/drones5020028>.
- Lindgren, F., Rue, H., Lindström, J., 2011. An explicit link between Gaussian fields and Gaussian Markov random fields: the stochastic partial differential equation approach. *J. R. Stat. Soc. Ser. B Stat. Methodol.* 73, 423–498.
- Lopez, G.R., Levinton, J.S., 1987. Ecology of deposit-feeding animals in marine sediments. *Q. Rev. Biol.* 62, 235–260.
- Mancini, G., Casoli, E., Ventura, D., Jona-Lasinio, G., Criscoli, A., Belluscio, A., Ardizzone, G.D., 2019. Impact of the Costa Concordia shipwreck on a *Posidonia oceanica* meadow: a multi-scale assessment from a population to a landscape level. *Mar. Pollut. Bull.* 148, 168–181. <https://doi.org/10.1016/j.marpolbul.2019.07.044>.
- Mancini, G., Casoli, E., Ventura, D., Jona-Lasinio, G., Belluscio, A., Ardizzone, G.D., 2021. An experimental investigation aimed at validating a seagrass restoration protocol based on transplantation. *Biol. Conserv.* 264. <https://doi.org/10.1016/j.biocon.2021.109397>.
- Martino, S., Pace, D.S.D.S., Moro, S., Casoli, E., Ventura, D., Frachea, A., Silvestri, M., Arcangeli, A., Giacomini, G., Ardizzone, G., Jona-Lasinio, G., 2021. Integration of presence-only data from several sources: a case study on dolphins'

- spatial distribution. *Ecography* 44, 1533–1543. <https://doi.org/10.1111/ecog.05843>.
- Massin, C., Doumen, C., 1986. Distribution and feeding of epibenthic holothuroids on the reef flat of Laing Island (Papua New Guinea). *Mar. Ecol. Prog. Ser.* 185–195.
- Mercier, A., Gebruk, A., Kremetskaia, A., Hamel, J.-F., 2024. An overview of taxonomic and morphological diversity in sea cucumbers (Holothuroidea: Echinodermata). *World Sea Cucumbers*, pp. 3–15.
- Neofitou, N., Lolas, A., Ballios, I., Skordas, K., Tziantziou, L., Vafidis, D., 2019. Contribution of sea cucumber *Holothuria tubulosa* on organic load reduction from fish farming operation. *Aquaculture* 501, 97–103. <https://doi.org/10.1016/j.aquaculture.2018.10.071>.
- Pasquini, V., Porcu, C., Marongiu, M.F., Follesa, M.C., Giglioli, A.A., Addis, P., 2022. New insights upon the reproductive biology of the sea cucumber *Holothuria tubulosa* (Echinodermata, Holothuroidea) in the Mediterranean: implications for management and domestication. *Front. Mar. Sci.* 9, 1–16. <https://doi.org/10.3389/fmars.2022.1029147>.
- Piazza, P., Cummings, V., Guzzi, A., Hawes, I., Lohrer, A., Marini, S., Marriott, P., Menna, F., Nocerino, E., Peirano, A., 2019. Underwater photogrammetry in Antarctica: long-term observations in benthic ecosystems and legacy data rescue. *Polar Biol.* 42, 1061–1079.
- Price, A.R.G., Harris, A., McGowan, A., Venkatachalam, A.J., Sheppard, C.R.C., 2010. Chagos feels the pinch: assessment of holothurian (sea cucumber) abundance, illegal harvesting and conservation prospects. In: *British Indian Ocean Territory*.
- Price, D.M., Robert, K., Callaway, A., Lo Iacono, C., Hall, R.A., Huvenne, V.A.I., 2019. Using 3D photogrammetry from ROV video to quantify cold-water coral reef structural complexity and investigate its influence on biodiversity and community assemblage. *Coral Reefs* 38, 1007–1021. <https://doi.org/10.1007/s00338-019-01827-3>.
- Purcell, S.W., Conand, C., Uthicke, S., Byrne, M., 2016a. Ecological roles of exploited sea cucumbers. In: *Oceanography and Marine Biology*. CRC Press, pp. 375–394.
- Purcell, S.W., Hair, C.A., Mills, D.J., 2012. Sea cucumber culture, farming and sea ranching in the tropics: progress, problems and opportunities. *Aquaculture* 368, 68–81.
- Purcell, S.W., Piddocke, T.P., Dalton, S.J., Wang, Y.-G., 2016b. Movement and growth of the coral reef holothuroids *Bohadschia argus* and *Thelenota ananas*. *Mar. Ecol. Prog. Ser.* 551, 201–214.
- Purcell, S.W., Rallings, S.L., Hammond, A.R., 2023. Long-term home ranging in the large sea cucumber, *Holothuria fuscopunctata*. *Coral Reefs* 42, 1059–1066. <https://doi.org/10.1007/s00338-023-02413-4>.
- Purcell, S.W., Shea, S.K.H., Gray, B.C.T., 2025. Decadal changes in value of dried sea cucumbers (bêche-de-mer) in Hong Kong markets. *Mar. Policy* 171, 106450.
- Rakaj, A., Fianchini, A., 2024. Mediterranean sea cucumbers—biology, ecology, and exploitation. In: *The World of Sea Cucumbers*. Elsevier, pp. 753–773.
- Rakaj, A., Fianchini, A., Boncagni, P., Lovatelli, A., Scardi, M., Cataudella, S., 2018. Spawning and rearing of *Holothuria tubulosa*: a new candidate for aquaculture in the Mediterranean region. *Aquac. Res.* 49, 557–568.
- Rakaj, A., Morrioni, L., Grosso, L., Fianchini, A., Pensa, D., Pellegrini, D., Regoli, F., 2021. Towards sea cucumbers as a new model in embryo-larval bioassays: *Holothuria tubulosa* as test species for the assessment of marine pollution. *Sci. Total Environ.* 787, 147593.
- Ram, R., Chand, R.V., Southgate, P.C., 2016. An overview of sea cucumber fishery management in the Fiji Islands. *J. Fish. Aquat. Sci.* 11, 191–205.
- Shiell, G.R., Knott, B., 2010. Aggregations and temporal changes in the activity and bioturbation contribution of the sea cucumber *Holothuria whitmaei* (Echinodermata: Holothuroidea). *Mar. Ecol. Prog. Ser.* 415, 127–139.
- Sicuro, B., Levine, J., 2011. Sea cucumber in the Mediterranean: a potential species for aquaculture in the Mediterranean. *Rev. Fish. Sci.* 19, 299–304.
- Siegenthaler, A., Cánovas, F., González-Wangüemert, M., 2015. Spatial distribution patterns and movements of *Holothuria arguinensis* in the Ria Formosa (Portugal). *J. Sea Res.* 102, 33–40. <https://doi.org/10.1016/j.seares.2015.04.003>.
- Simpson, D., Illian, J.B., Lindgren, F., Sørbye, S.H., Rue, H., 2016. Going off grid: computationally efficient inference for log-Gaussian Cox processes. *Biometrika* 103, 49–70.
- Slater, M., Chen, J., 2015. Sea cucumber biology and ecology. *Echinoderm Aquac* 47–55. <https://doi.org/10.1002/9781119005810.ch3>.
- Uthicke, S., 2001. Nutrient regeneration by abundant coral reef holothurians. *J. Exp. Mar. Biol. Ecol.* 265, 153–170.
- Uthicke, S., Benzie, J., 2001. Effect of bêche-de-mer fishing on densities and size structure of *Holothuria nobilis* (Echinodermata: Holothuroidea) populations on the Great Barrier Reef. *Coral Reefs* 19, 271–276.
- Vafidis, D., Antoniadou, C., 2023. Holothurian fisheries in the hellenic seas: seeking for sustainability. *Sustainability* 15, 9799.
- Ventura, D., Grosso, L., Pensa, D., Casoli, E., Mancini, G., Valente, T., Scardi, M., Rakaj, A., 2023. Coastal benthic habitat mapping and monitoring by integrating aerial and water surface low-cost drones. *Front. Mar. Sci.* 9, 1–15. <https://doi.org/10.3389/fmars.2022.1096594>.
- Ventura, D., Mancini, G., Casoli, E., Pace, D.S., Lasinio, G.J., Belluscio, A., Ardizzone, G., 2022. Seagrass restoration monitoring and shallow-water benthic habitat mapping through a photogrammetry-based protocol. *J. Environ. Manag.* 304, 114262. <https://doi.org/10.1016/j.jenvman.2021.114262>.
- Williamson, J.E., Duce, S., Joyce, K.E., Raouf, V., 2021. Putting sea cucumbers on the map: projected holothurian bioturbation rates on a coral reef scale. *Coral Reefs* 40, 559–569.
- Williamson, L.D., Scott, B.E., Laxton, M., Illian, J.B., Todd, V.L.G., Miller, P.I., Brookes, K.L., 2022. Comparing distribution of harbour porpoise using generalized additive models and hierarchical Bayesian models with integrated nested laplace approximation. *Ecol. Model.* 470, 110011.
- Wolfe, K., Byrne, M., 2017. Biology and ecology of the vulnerable holothuroid, *Stichopus herrmanni*, on a high-latitude coral reef on the Great Barrier Reef. *Coral Reefs* 36, 1143–1156. <https://doi.org/10.1007/s00338-017-1606-5>.
- Yuan, Y., Bachl, F.E., Lindgren, F., Borchers, D.L., Illian, J.B., Buckland, S.T., Rue, H., Gerrodette, T., 2017. Point Process Models for Spatio-Temporal Distance Sampling Data from a Large-Scale Survey of Blue Whales.